

Structural and Electrical Properties of PVA/PVP Blend Doped with Methylene Blue Dye

H. M. Zidan¹, N. A. El-Ghamaz¹, A. M. Abdelghany², A. Lotfy^{3,*}

¹ Physics Department, Faculty of Science, Damietta University. P.O.Box 34517, New Damietta, Egypt.

² Spectroscopy Department, Physics Division, National Research Center, 33 ElBehouth St., Dokki, 12311, Cairo, Egypt.

³ Department of Basic Science, Higher Institute of Engineering and Technology, New Damietta, Egypt.

* E-mail: ahmedwaves20@yahoo.com

Received: 19 July 2016 / Accepted: 6 September 2016 / Published: 10 October 2016

Films of PVA/PVP blend (1:1) doped with different levels of methylene blue dye (MB) were prepared using the casting technique. X-ray, IR, DC and AC analyses were used to give more information about structural variation that arises due to different doping levels. Semi-crystalline nature of PVA/PVP blend revealed from X-ray diffraction pattern. The crystallinity of the doped blends decays as the doping level of MB increases. The IR analysis showed that a presence of double bond segments which are assumed as an appropriate sites for polarons and/or bipolarons. The dependence of the DC electrical conduction on the temperature was ascribed in view of phonon–assisted interpolymer one–dimensional hopping of charge carriers. Dielectric analysis showed that the values of ϵ_r decrease with increasing frequency and becomes constant at higher frequencies. On the other hand, ϵ_r increases with the temperature. The σ_{ac} values increase with increasing the frequency as well as MB content. The values of the frequency exponent S designate that quantum mechanical tunneling mechanism (QMT) is the dominant model within prepared samples.

Keywords: PVA/PVP blend; XRD; FTIR; electrical conductivity.

1. INTRODUCTION

During last decades polymeric containing materials attracted the attention of scientists for widespread applications such as solar energy conversion, coatings, adhesives, lithography, light-emitting diodes, sensors, laser development and many applications. [1, 2]. Doping of polymers permits person to get novel material with superior properties [3, 4]. In recent years dye doped polymers have attracted attention of materials scientist due to their optical and electrical characteristics which can be controlled by doping process for specific uses and applications [5]. Azo dyes doped polymers have been investigated extensively due to their interesting properties such as the possible application in

nonlinear optical devices, optical communication, optical storage, information processing and particularly all optical modulators.

Poly (vinyl alcohol) (PVA) is one of the superior polymeric matrices results from the widespread industrial applications. For instance, when doped with phosphoric acid it can be used as a solid polymer electrolyte in solid state electro chromic displays and solid state photocells [6]. PVA, as a semi-crystalline materials, displays unique physical character subsequent from crystal-amorphous interfacial effects [7,8].

Polyvinyl pyrrolidone (PVP) is a conjugated polymer gains its importance from its moderate electrical conductivity, environmental stability and ease of processing. Moreover, PVP and PVA are miscible water-soluble materials in almost all ratios [9].

Polyblends have attracted the physicist due to their fascinated properties which may be modified to a specific needs by the process of blending [10]. PVP/PVA polymeric blend is probable materials that have good charge storage capacity and sensitive for dopant addition [11]. The PVP influence on PVA crystallinity and optical band gap have been investigated by Saudha Kamath et al [12]. They reported that the crystallinity of PVA/PVP blends decreases with increasing the level of PVP and PVA (50) wt % / PVP (50) wt % is more stable and suitable samples for investigation due to its brittleness. The structural, thermal, optical, and electrical properties of PVA/PVP polymer blend can be appropriately modified by addition of different dopants depending on their reactivity with the host matrix [11-16].

Many authors [15-17] reported on the doped polyblend of PVA/PVP films while very few works are available on PVA/PVP doped with dye. Previous studies of our research group devoted for investigation of filling level and nature of metal halide effect on the structural modifications of different polymeric matrices including PVA films [17]. The manuscript aims to describe the interaction and structural modifications result from minor addition in the doping level of MB to PVA/PVP blend and change in the physical properties using XRD, FTIR and AC electrical measurements.

2. EXPERIMENTAL

2.1. Materials and sample preparation

The polyvinyl alcohol (PVA) Merck-Germany with molecular weight 14000, polyvinyl pyrrolidone (PVP) Aldrich-England with molecular weight 40000, Methylene blue (MB) Mumbai-India was purchased and used as received. The molecular structure of PVA, PVP and Azo dye (methylene blue) are shown in Fig.1.

Equal weights of PVA and PVP (1:1) were dissolved in doubly distilled water at 50 °C with continuous stirring until complete dissolution. Azo dye (methylene blue) with different weight fractions were added to the polymeric solution of suitable viscosity and stirred vigorously for 2 hours to ensure complete interaction and homogeneity. Prepared sample were labeled as indicated in Table 1. The blends with different azo dye levels were then casted in serialized Petri dishes. Prepared samples were dried in an incubator at 50 °C for 2 days. Dried samples peeled from Petri dishes and kept in a

desiccator until use. The thickness of the obtained films are in the range $\sim 0.1 - 0.2$ mm. The dopant level (wt %) was pre-calculated using equation (1);

$$W(\text{wt}\%) = \frac{W_d}{W_p + W_d} \times 100, \quad (1)$$

where W_p and W_d represent the weight of polymer and dopant respectively.

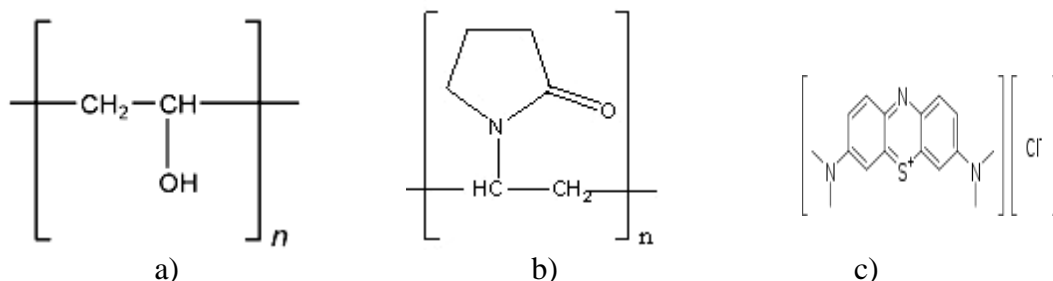


Figure 1. The molecular structure of (a) PVA, (b) PVP and (c) methylene blue (MB).

2.2. Physical measurements:

X-ray diffraction (XRD) scans were performed using Philips diffractometer with Cu k_{α} -radiation ($\lambda = 1.540 \text{ \AA}$). The tube operated at 30 kV and Bragg's angle (2θ) in the range $5 - 60^{\circ}$. Infrared (IR) measurements in the wavenumber range $4000 - 400 \text{ cm}^{-1}$ were carried out using Nicolet *is10* single beam Fourier transform-infrared spectrometer. DC electrical measurements were performed by [Keithley 175 with an accuracy $\pm 2\%$]. AC electrical measurements were performed with using a programmable automatic LCR meter [model Hioki 3531 Z Hitester] in the frequency range 50 Hz - 3.5 MHz. Both of DC and AC measurements were performed in the temperature range 300 - 380 K in a specially designed cell. Samples placed between two polished circular copper plates for good contact. The temperature was controlled and measured by Cole-Plimer temperature controller model R/S. The temperature was measured using NiCr-NiAl thermocouple.

3. RESULTS AND DISCUSSION

3.1. X-ray diffraction pattern

Fig. 2a displays the X-ray diffraction pattern of pristine PVA/PVP polyblend and PVA/PVP doped with different concentrations of MB. XRD pattern reveals nearly same behavior with a main broad diffraction peak observed at $2\theta \approx 20^{\circ}$ which may be attributed to the semi-crystalline nature of the prepared pristine blend corresponding to (110) plane. It can be also observed that, the peak position is slightly shifted to lower 2θ while the intensity decreases with gradient increase in MB content. This may be interpreted in terms of the strong interaction between polymer blend and filler which results in the degree of intermolecular interaction, which implied a change in the degree of crystallization combined with increases in the amorphous regions [18]. This behavior demonstrates the complexation

between the MB and polymeric matrix [19, 20]. This increase in the amorphous regions causes reduction in the energy barrier and segmental motion of the polymer resulting in a higher ionic conductivity [21]. There are no peaks observed in the XRD spectra related to the MB (Fig. 2b) which indicates formation of polymer blend free from crystalline methylene blue dye and complete miscibility of the dye. This also supports the interaction process between MB and PVA/PVP blend.

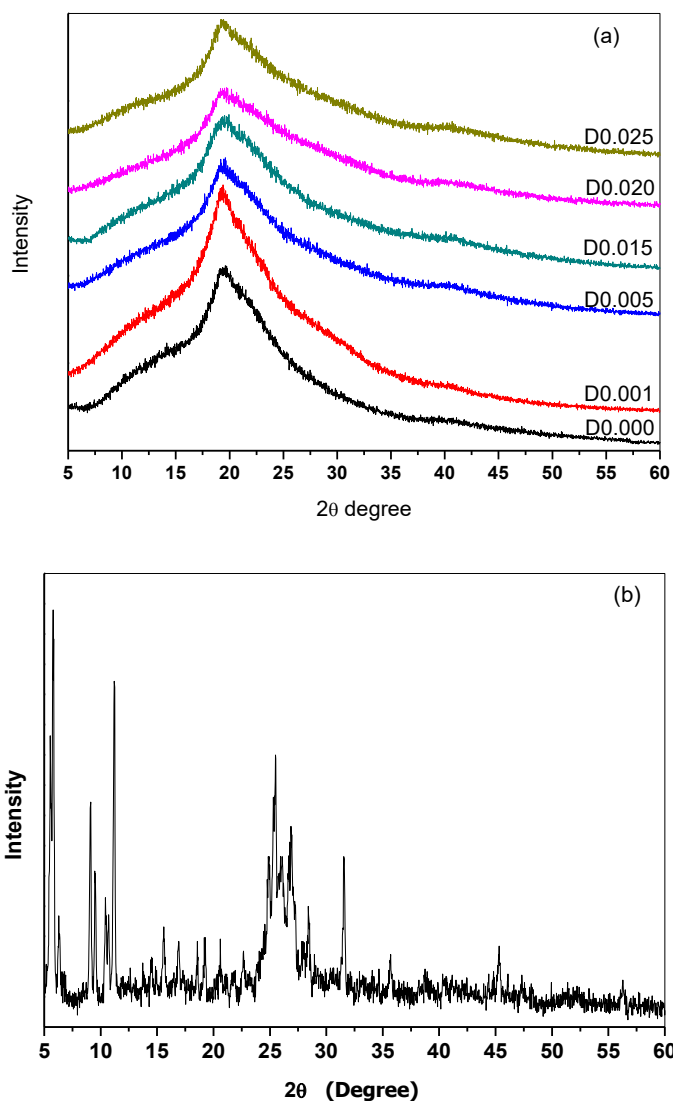


Figure 2. X-ray diffraction scan of (a) PVA/PVP blend doped with different levels of MB and (b) pristine methylene blue (MB) powder.

From the width of the XRD peak, the mean crystalline size of the present system can be calculated using Debye-Scherer's equation [22] and tabulated in Table 1.

$$D = \frac{K\lambda}{\beta \cos\theta} \tag{2}$$

where β is the angular full width at half maximum (FWHM) corresponding to Bragg angle θ (in degrees), D is the average crystalline size, K defined as shape factor that varies between ($0.89 < K < 1$) [20] and λ is the wavelength of used X-ray (1.540 \AA). It is observed that, there is small effect of

change of MB content on the average crystallite size of PVA/PVP blend which has values in the range 9.48 - 9.16 nm (Table 1).

Table 1. Sample composition and average crystalline size for poly blend with different levels of MB.

Sample	MB content (Wt%)	D (nm)
D0.000	0.000	9.29
D0.001	0.001	9.16
D0.005	0.005	9.41
D0.015	0.015	9.04
D0.020	0.020	9.43
D0.025	0.025	9.48

3.2. FTIR absorption spectra

FTIR spectroscopic unique technique used for investigation of the vibrational spectra results from variations in chemical compositions, chemical interaction and variations in functional group during interaction [23]. Information pertaining to ion-polymer interaction and molecular structure can be obtained from FTIR studies. If there is any interaction, the vibrational modes of the function groups give shift in its wavenumbers and the peaks intensity. Polymers can interact with each other or with certain dopants from secondary bonding, i.e, hydrogen bonding.

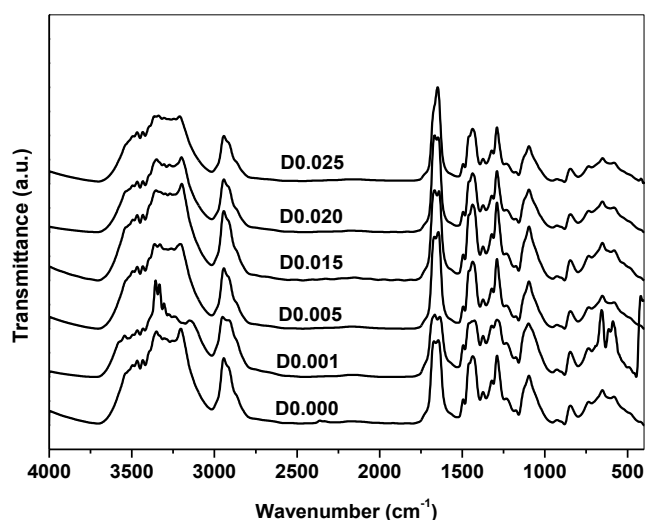


Figure 3. FTIR spectra of PVA/PVP blend doped with different levels of MB.

Fig. 3 shows the FTIR spectra of pure PVA/PVP blend and PVA/PVP blend doped with different doping levels of MB at room temperature in the region 400 - 4000 cm^{-1} . Almost all the vital bands obtained from PVA and PVP spectrum are present. The spectra are in good agreement with that reported previous [24]. The observed absorption spectra display characteristic bands of stretching and bending vibrations of the functional groups within the samples. The absorption band positions and its

assignments for characteristic bands are listed in Table 2. It is noticed that, in case of PVA/PVP doped with MB, the spectra show shifts in some bands and changes in the intensity of other bands taking into account pristine blend films. This indicates the considerable interaction between the blend and dye. The absorption peak at 1680 cm^{-1} was assigned to C=C stretching vibration while the peak at 1080 cm^{-1} was assigned to the carbonyl group (C=O). The intensity of such peaks is sensitive to the doping level of MB dye. It is noted that the presence of such double bond are correlated with a suitable sites for polarons and/or bipolarons [25].

Table 2. Assignments of the IR characteristic peaks of PVA/PVP blend doped with different levels of MB.

Wavenumber (cm^{-1})	Assignment
830	OH stretching
910	Syndiotacticity of PVA
1080	C = O stretching
1250	C – O – C stretching
1280	CH ₂ bending or C = C stretch
1430	C = C stretching
1480	CH ₂ bending
1680	C = C stretching
2950	CH ₂ asymmetric stretching
3400	OH stretching

3.3. DC electrical conductivity

The dc electrical conductivity σ_{dc} values can be calculated from the following equation

$$\sigma_{dc} = \frac{L}{R.A}, \quad (3)$$

where L is the thickness in cm, A is the surface area in cm^2 and R is the resistance in ohm of the sample.

The temperature dependence of dc conductivity measurements were investigated in the temperature range 303 - 363 K. Fig. 4 represents the dependence of $\ln \sigma_{dc}$ on the reciprocal of the absolute temperature for films of pure PVA/PVP blend and PVA/PVP blend doped with different levels of MB. It is noticed that the conductivity of all samples increases with increasing the temperature due to increasing in free volume and their respective ionic and segmental mobility [26]. Also, it is obvious that the electrical conductivity of the MB doped samples are greater than that of pure PVA/PVP blend and increases as increasing the MB doping levels. This result suggests the choice of MB as a dopant to improve the electrical conductivity of PVA/PVP blend. The improvement of σ_{dc} as a result of MB doping is in agreement with the results obtained by Mahendia et al. [27]. This could be interpreted as; the reduction of the crystalline phase due to MB doping (reported in X-ray section) leads to decreasing in the interfacial barrier and subsequently increase the transition mobility of electron hopping across the barrier. This in turn provides a conducting path through the amorphous region of the polymer matrix resulting in enhanced conductivity.

The linear variation of $\ln \sigma_{dc}$ with reciprocal temperature for the present system (Fig. 4) suggests an Arrheniuseas relation behavior; [28]

$$\sigma_{dc} = \sigma_o \exp (-\Delta E_{dc} / k_B T) \tag{4}$$

where σ_o is the proportionality constant, ΔE_{dc} is the activation energy, k_B is the Boltzmann constant and T is the absolute temperature. From this equation the activation energy ΔE_{dc} of the present system can be calculated and is found to be in the range 0.08 – 0.1 eV. It is also found that the values of ΔE_{dc} slightly decrease as the doping level of MB increase.

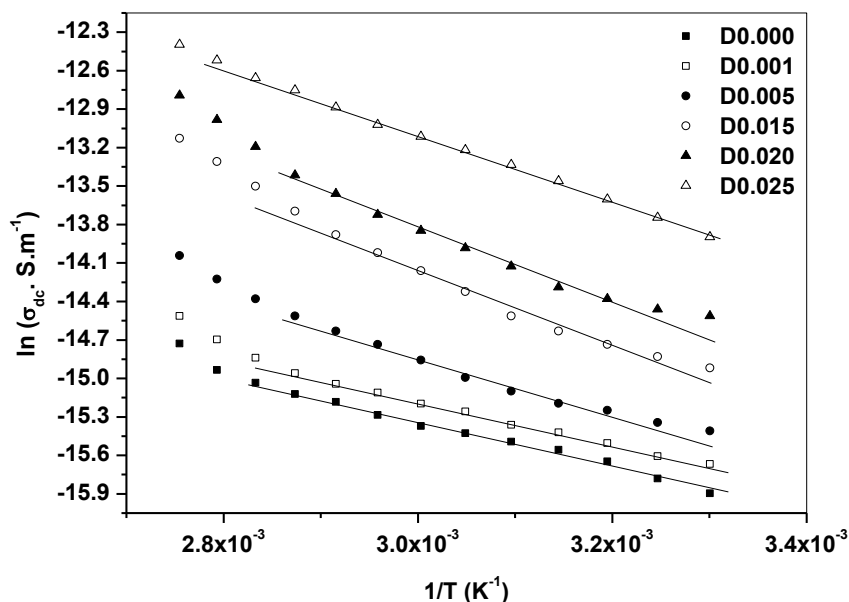


Figure 4. The dependence of $\ln \sigma_{dc}$ on the reciprocal absolute temperature for PVA/PVP blend doped with different levels of MB.

The conjugated double bonds, detected by IR analysis in the present work (section 3.2) may be assumed to be suitable cause for presence of polarons and/or bipolarons in the studied polymeric matrix doped with MB dye. Kuivalainen modified interpolaron hopping model can be applied to study the dc conduction mechanisms on the origin of phonon–assisted hopping of charge carriers bound states in the studied polymeric system [29]. In view of this model, the electrical conductivity can be expressed as

$$\sigma = \frac{Ae^2\gamma(T)^2}{KT} \frac{\zeta}{R_o^2} \frac{y_p y_{bp}}{(y_p + y_{bp})^2} \exp\left(\frac{-2BR_o}{\zeta}\right) \tag{5}$$

where k_B is the Boltzmann's constant, A and B are constant (0.45, 1.39 respectively), Y_p and y_{bp} are the levels of polarons and bipolarons, $R_o = (3/(4\pi C_{imp}))^{1/3}$ is the distinctive separation between impurities whose level is C_{imp} , $(\xi_{||} \xi_{\perp}^2)$ is the average decay length of a polaron or bipolaron wave function with $\zeta_{||}$ and ζ_{\perp} are the decay lengths parallel and perpendicular to the polymer chain. Breads et al. [30] shows that both polaron and bipolaron induces defect to the some extension. Thus, electronic transition are given by;

$$\gamma(T) = \gamma_o (T/300 K)^{11}, \tag{6}$$

where $\gamma_o = 1.2 \times 10^{17} S^{-1}$ [31].

The value of dc conductivity σ_{dc} was attained in view of fitting parameter C_{imp} , $\zeta_{\parallel} = 1.06$ nm, and $\zeta_{\perp} = 0.22$ nm [32] that depends on the inter-chain distance and inter-chain resonance energy [33]. Taking $y_p = y_{bp}$ and using equations 5 and 6, the values of hopping distance R_o of the charge carriers which is considered as the separation between impurities can be calculated.

Fig. 5 represents the temperature dependence of the calculated values of R_o for PVA/PVP with various doping levels of MB. It is found that there is a linear decrease of R_o as the temperature increases for all samples. This suggests that the thermally activated polarons and / or bipolarons (acting as hopping centers for the charge carriers) increases with increasing temperature.

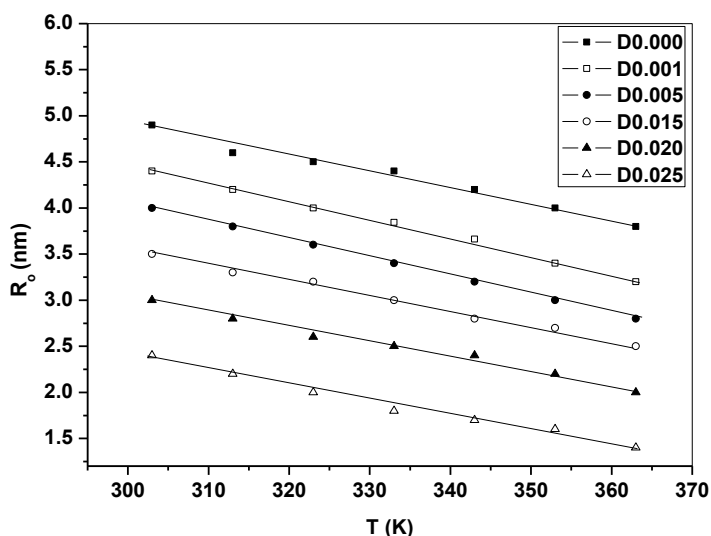


Figure 5. The temperature dependence of R_o for various doping levels of MB dye.

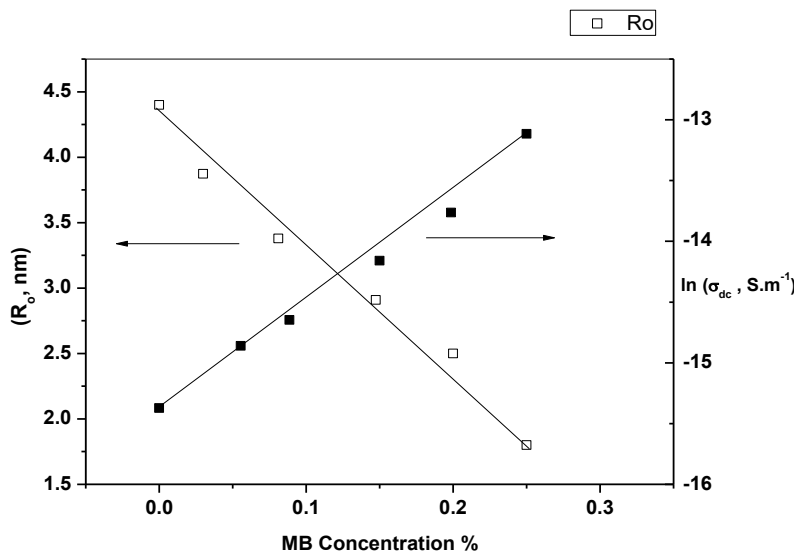


Figure 6. The effect of doping level with MB on R_o and $\ln \sigma_{dc}$ for PVA/PVP at constant temperature $T = 333$ K.

The effect of doping level with MB on $\ln \sigma_{dc}$ and R_o at constant temperature ($T = 333$ K) for PVA/PVP is plotted in Fig. 6. It can be found that $\ln \sigma_{dc}$ increases while R_o decreases as doping level

increases. This result is in agreement with the results obtained from the doping level dependence of the intensity of the band at 1680 cm^{-1} which was assigned to C = C vibrating mode (in IR section). This assumption indicates a local site of vibrations which may be considered as suitable hopping centers for charge carriers of the electrical conduction. Previous assumptions support application of the present conduction model.

It is noteworthy that the obtained values of R_0 for the present system are in the range 1.5 - 5 nm. Considering the minimum monomer unit length to be 0.25 nm [34], the hopping distance is in the range of 6 to 20 times the monomer unit lengths. Hence, the present conduction mechanism is of an intera-chain one-dimensional hopping type.

3.4. Dielectric properties

3.4.1. Variation of dielectric constant with frequency and temperature

Investigation of the dielectric properties of a material plays an important role in determining the suitable applications of this material [35]. The dielectric constant (permittivity) ϵ^* can be considered as a complex quantity and is given by

$$\epsilon^* = \epsilon_r - i \epsilon_i, \quad (7)$$

where ϵ_r is the real part of permittivity and ϵ_i is the imaginary one. The real dielectric constant, ϵ_r , can be deduced from the measured capacitance of the sample according to the following equation [36, 37]:

$$\epsilon_r = C_p d / \epsilon_0 A, \quad (8)$$

where C_p is the capacitance of the sample measured in parallel mode, ϵ_0 is permittivity of free space and d is the thickness of the sample. The imaginary part of the dielectric constant, ϵ_i , can be calculated using the calculated values of ϵ_r and the measured values of loss tangent ($\tan \delta$), using the equation [36, 37]:

$$\epsilon_i = \epsilon_r \tan \delta, \quad (9)$$

Both of C_p and $\tan \delta$ for all samples are measured in the frequency range 50 Hz -3.5 MHz and temperature range 303 - 373 K. The effect of doping of PVA/PVP blend with MB on both C_p and $\tan \delta$ at 333 K is shown in Fig. 7. The value of C_p and $\tan \delta$ are found to increase with increasing the doping level.

The dielectric permittivity as a function of frequency reflects the important effect of the MB content on the properties of pure PVA/PVP blend. The frequency dependence of ϵ_r and ϵ_i at $T = 333\text{ K}$ for samples D0.000 – D0.025 are shown in Figs 8 and 9 respectively. It is clear that ϵ_r and ϵ_i decrease with increasing frequency for all samples. The values of ϵ_r and ϵ_i are high at low frequency and decrease monotonically with increasing frequency until reaching to a constant value at higher frequencies. The high values of ϵ_r and ϵ_i may be due to the interfacial effects within the bulk of the sample and the electrode effects [38]. Also, it is known that for polar materials, the initial value of ϵ_r and ϵ_i is high, but as the frequency of the field is increased, the value begins to drop because the dipoles are not able to follow the field variations. At high frequencies, the periodic reversal of the electric field occurs so fast that there is no excess ion diffusion in the direction of the field. The

polarization due to the charge accumulation decreases, leading to a decrease in the value of ϵ_r and ϵ_i [39, 40]. It is noticed that the values of ϵ_r and ϵ_i for the doped samples are higher than that of pure PVA/PVP and increase with increasing the doping level for all the frequency range. The increase in ϵ_r and ϵ_i upon increasing MB content can be explained in terms of increasing the accumulated charge because of the polarization of polymer/ dopant interfaces. The polarization makes an additional contribution to the charge quantity. Fig. 10 illustrates the increase of both ϵ_r and ϵ_i with increasing the content of MB at frequency 500 Hz and $T = 333$ K.

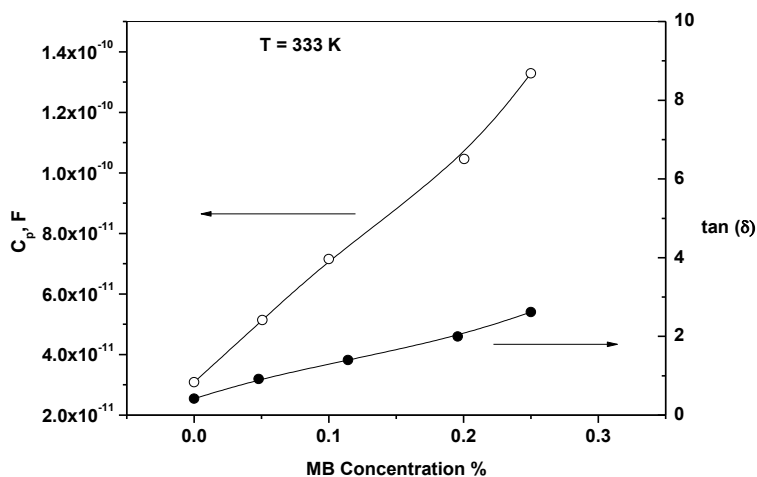


Figure 7. The effect of doping level with MB on C_p and $\tan \delta$ for PVA/PVP blend at $T = 333$ K.

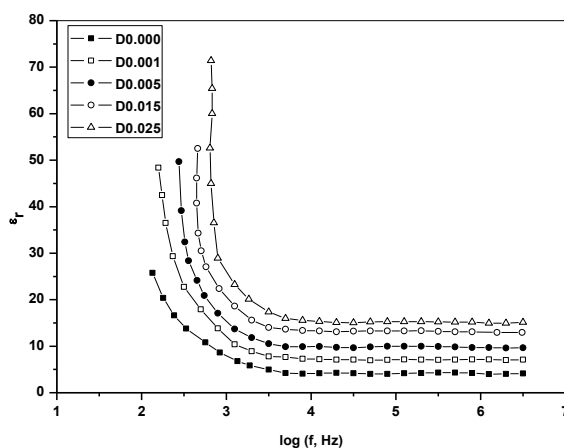


Figure 8. The frequency dependence of ϵ_r for PVA/PVP blend doped with different levels of MB at constant temperature 333 K.

From this point of view, the dielectric constant of the MB doped polymer will be higher than that of the pure polymer [41-43]. The temperature dependence of ϵ_r and ϵ_i for the samples D0.000 – D0.025 show that ϵ_r and ϵ_i increase with increasing temperature for all samples. The variation of ϵ_r with temperature is different for polar and non-polar polymers. In general, for non-polar polymers the

values of ϵ_r are independent of temperature but in the case of strong polar polymers, ϵ_r increases as the temperature increases. Moreover the increase in ϵ_r with temperature is due to greater freedom of movement of dipole molecular chain of polymer at high temperature. At lower temperature, as the dipoles are rigidly fixed in the dielectric, the field cannot change the condition of dipoles. As the temperature increases, the dipoles comparatively become free and they respond to the applied electric field. Thus, polarization increases and hence ϵ_r increases with the increase of temperature. One further effect may contribute to the increase of ϵ_r is the change in the intra and inter-molecular interactions which may involve the alignment or rotation of the dipoles present in the polymer with the increase of temperature [44].

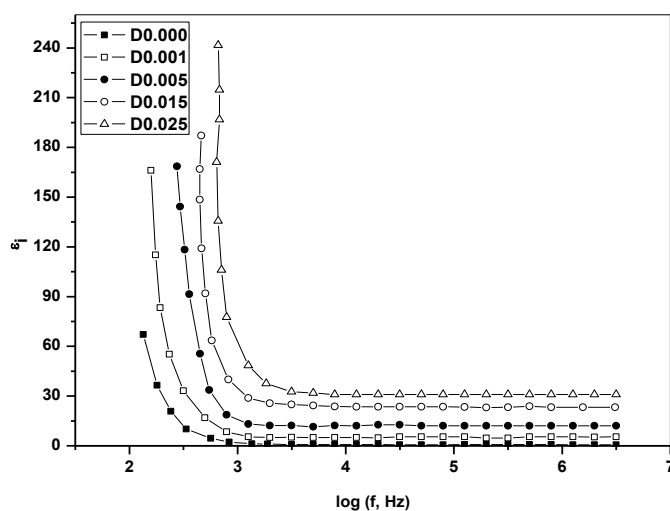


Figure 9. The frequency dependence of ϵ_i for PVA/PVP blend doped with different levels of MB at constant temperature 333 K.

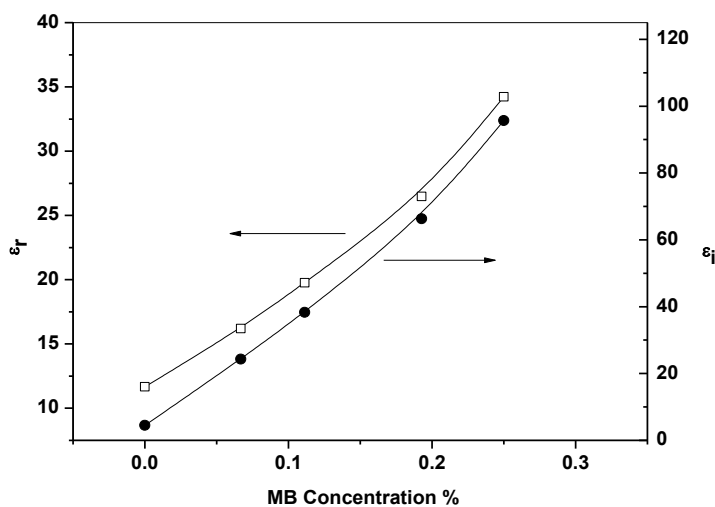


Figure 10. The effect of doping level with MB on ϵ_r and ϵ_i for PVA/PVP blend at $T=333$ K and $f = 500$ Hz.

3.4.2. AC conductivity

The ac conductivity can be obtained from the calculate values of ϵ_i , according to the relation: [45]

$$\sigma_{ac} = \omega \epsilon_0 \epsilon_i, \quad (10)$$

where $\omega = 2\pi f$ is the angular frequency. The natural logarithmic $\ln \sigma_{ac}$ as a function of the reciprocal temperature $1 / T$ at different frequencies in the frequency range 50 Hz – 3.5 MHz and temperature range 303 - 373 K for the present system is studied. It is found that all samples have the same behavior. Here we will present only the temperature dependence of $\ln \sigma_{ac}$ for the studied samples at two test frequencies 50 KHz and 3.5 MHz as shown in Fig. 11 (a,b). From this figure, it is noticed that the values of σ_{ac} increase with increasing the frequency and temperature. Also, the values of σ_{ac} increase with increasing the MB doping level. The increase in the values of σ_{ac} with increasing the frequency can be explained as follows. The increase in the oscillation field accompanied with increasing frequency will lead to an increase in the polarization of the samples appearing in that the form of conductivity increases. The behavior of σ_{ac} as a function of temperature can be explained according to the fact that the AC conductivity arises from the rapid transition between localized states of charged species such as electrons or dipoles [46].

The plots of σ_{ac} Versus $1 / T$ for blend doped with MB exhibit the same trend as that of pure blend. The values of σ_{ac} for the doped samples are higher than those obtained for pure blend due to the large dipole of MB content. This can attributed to the structural modification of polymeric matrix as a result of MB doping.

The temperature dependence of σ_{ac} is found to follow the Arrhenius relation which is given by:

$$\sigma_{ac} = \sigma_0 \exp (- \Delta E_{ac} / k_B T), \quad (11)$$

where ΔE_{ac} is the activation energy for ac electrical conduction. The values of ΔE_{ac} for PVA/PVP blend and that with different MB content at 50 KHz and 3.5 MHz are calculated and listed in Table 3. The relatively low values of ΔE_{ac} recommends the hopping or tunneling conduction mechanism for ac conduction for all samples.

Table 3. The dependence of the activation energy ΔE_{ac} for PVA/PVP blend on MB concentration

PVA/PVP blend	ΔE_{ac} (eV) at 50 KHz	ΔE_{ac} (eV) at 3.5 MHz
D0.000	0.32	0.42
D0.001	0.30	0.40
D0.005	0.29	0.39
D0.015	0.27	0.37
D0.025	0.25	0.35

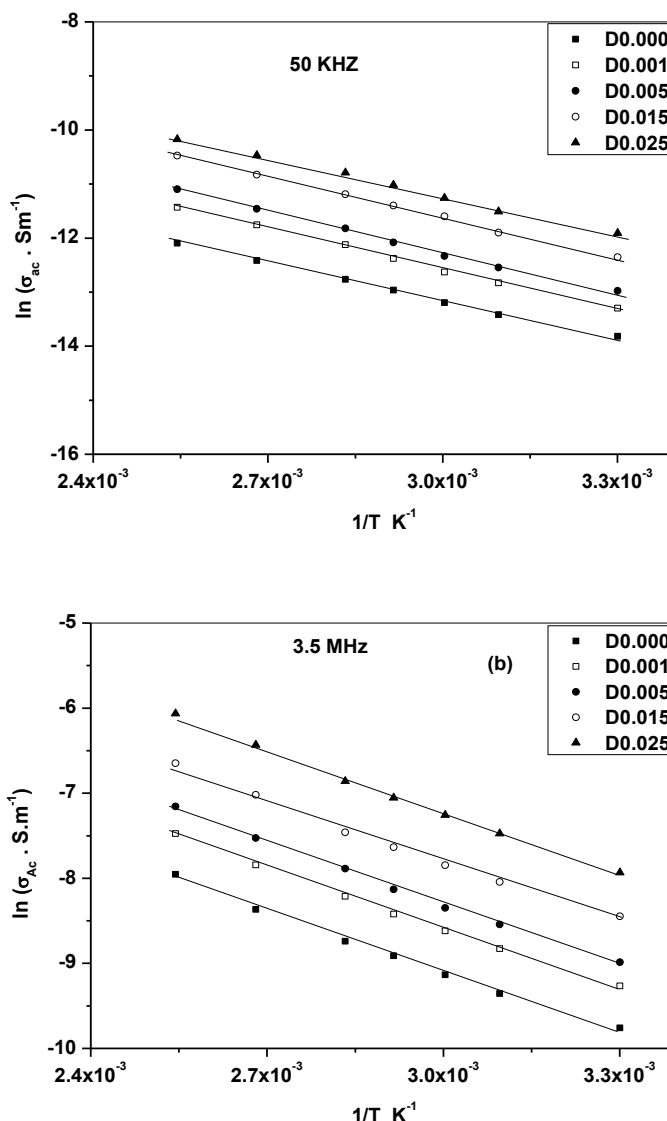


Figure 11. (a,b) The relation between $\ln \sigma_{ac}$ and $1/T$ for PVA/PVP blend doped with MB at $f = 50$ KHz and $f = 3.5$ MHz.

To investigate the dominant conduction mechanism, the frequency dependence of σ_{ac} can be analyzed according to the relation

$$\sigma_{ac} = A \omega^s, \tag{12}$$

where A is a constant, ω is the angular frequency and s is an exponential power. The value and behavior of S with temperature can give information about the dominant conduction mechanism. The value of S is the slope of the straight line portion of the relation between $\log \sigma_{ac}$ and $\log \omega$ [Fig. 12]. Fig. 13 illustrates the dependence of S on the temperature for all the studied samples. It is clear that for pure PVA/PVP blend the values of S is near unity and are independent on temperature. On the other hand the values of S slightly decrease with increasing MB level in PVA/PVP matrix and remain near unity. Moreover, this behavior recommends the quantum mechanical tunneling conduction mechanism to be the dominant mechanism for ac conduction.

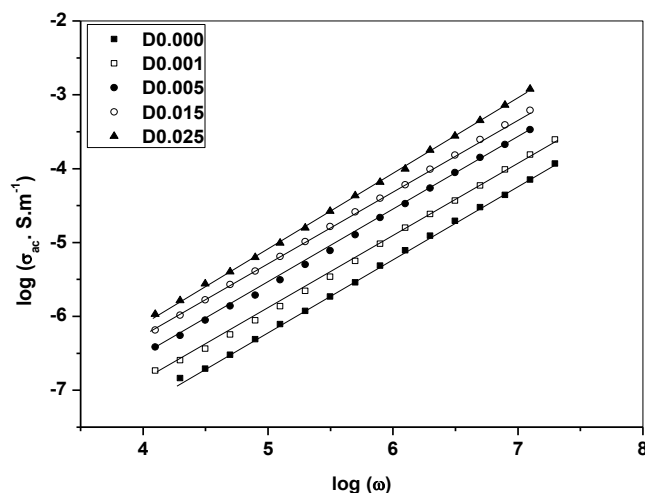


Figure 12. The relation between $\log \sigma_{ac}$ and $\log \omega$ for PVA/PVP blend doped with MB at test temperature 333 K.

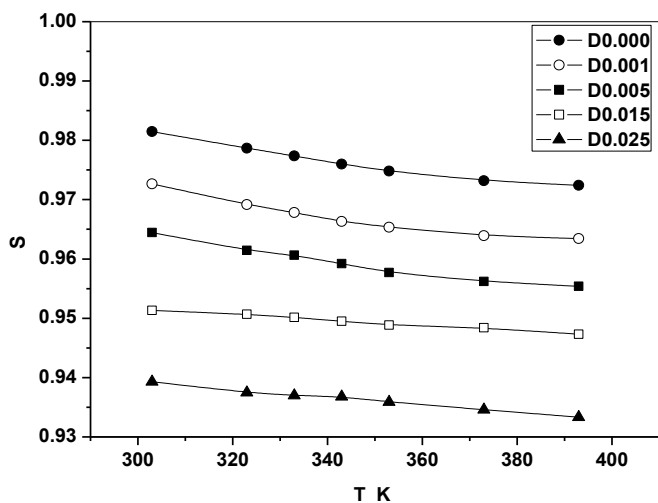


Figure 13. The dependence of S on temperature for PVA/PVP blend doped with MB.

4. CONCLUSIONS

Pristine samples of equi-mass poly-blend (PVA/PVP) and same sample with different doping concentration of MB dye were prepared and studied. Obtained data shows significant changes in the measured physical parameters after doping with MB. Observed changes can be interpreted in terms of the structural modifications in polymeric matrices after doping result from defect formation. The X-ray analysis showed that no significant peaks, characterizing MB crystals, were detected. The degree of crystallinity of the main phase, detected by X-ray diffraction, decreases with increasing the doping level of MB indicating changes in the degree of crystallinity. This behavior establishes a type of interaction between MB and polymeric matrices. FTIR spectroscopic analysis showed the presence of

certain characteristic bands (double bond), which assigned to polarons and/or bipolarons and suggests a one dimensional electrical conduction mechanism. DC electrical conductivity displayed that the conductivity of the present system increases with increasing of both temperature and the MB doping level. The modified interpolaron hopping model of Kuvalainem was used to describe the electrical conduction mechanism. The hopping distance (R_0) was found to decay as a function of both temperature and content of MB. The values of ϵ_r decrease with increasing frequency and attain constant values at higher frequencies which may be attributed to the relation between electric dipoles and field variations. The values of ϵ_r increase with MB doping due to the induced increase in free volume offered by the large size of MB molecule. Also, the quantity of the amassed charges will increase due to the resultant polarization at polymer/dopant interfaces.

References

1. M. Teroda, Y. Ohaba, *J. Appl. Phys.*, 22 (1983) 1392.
2. K. Shunichi, *Radiat. Phys. Chem.*, 27 (1986) 65.
3. H. M. Zidan, and M. Abu-Elnader, *Physica B*, 355 (2005) 308.
4. H. M. Zidan, *J. Polym. Sci B. Polym. Phys.*, 41 (2003) 112.
5. H. M. Zidan, A. El-Khodary, I. A. El-Sayed, H. I. El-Bohy, *Journal of Applied Polymer Science*, 117(2010)1416.
6. E.M. Abdelrazek, I.S. Elashmawi, A. El-Khodary, A. Yassin, *Current Applied Physics*, 10(2010) 607.
7. I. Su, Z.Y.Ma, J.I.Scheinbeim, B.A.Newman, *J. Polym. Sci. Polym. Phys.*, 33 (1995) 85.
8. A.Tawansi, H. M. Zidan, *J. Phys. D Apple. Phys.*, 23 (1990) 1320.
9. C.V.S. Reddy, X. Han, Q.Y. Zhu, L.Q. Mai, W. Chen, *Microelectron. Eng.*, 83 (2006) 281.
10. H. M. Zidan, A. Tawansi, M. Abu-Elnader, *Physica B*, 339 (2003)78.
11. H.M. Ragab. *Physica B*, 406 (2011) 3759.
12. M.K. Sudha Kamath, H.G. Harish kumar, R. Chandramani, M.C. Radhakrishna, *Archives of Physics Ressearch*, 6 (2) (2015) 18.
13. I.S. Elashmawi, E.M. Abdelrazek, A.Yassin, *British Journal of Applied Science &Technology*, 4 (30) (2014) 4263.
14. K. Hemalatha, H. Somashekarappa, R. Somashekar, *Advances in Materials and Chemistry*, 5 (2015) 408.
15. E.M. abdelrazek and H.M. Ragab, *Indian J. Phys.*, 89 (6) (2015) 577.
16. N. Rajeswari, S. Selvasekarapandian, C. Sanjeeviraja, J. Kawamura, S. Asath Bahadur, *Polym. Bull.*, 71 (2014) 1061.
17. H.M. Zidan, *Journal of Applied Polymer Science*, 88(2003) 516.
18. R.M. Hodye, G.H. Edward, G.P. Simon, *Polymer*, 37 (1996) 1371.
19. N. Rajeswari, S. Selvasekarapandian, S. Karthikeyan, C. Sanjeeviraja, Y. Iwaia, J. Kawamura, *Ionics*, 19 (2013) 1105.
20. S. Singh, H. Kaur, D. Pathak and R. K. Bedi, *Digist. J. Nanometer and Biostructure*, 6 (2011) 689.
21. R. Baskaran, S. Selvasekarapandian, N. Kuwata, J. Kawamura, T. Hattori, *Solid State Ionics*, 177 (2006) 2679.
22. I.S. Elashmawi, A.M. Abdelghany, N.A. Hakeem. *J Mater Sci: Mater. Electron*, 24 (2013) 2956.
23. A.E.B. Vladimir, R.R.M. Jose, V.P.A. Nancy, A.E. Guillermo, L.D.R. Jose, *Materials Science, Engineering and Technology*, In Tech Infrared Spectroscopy (2012) 195.
24. A.M. Abdelghany, E.M. Abdelrazek, D.S. Rashad, *Spectrochimica Acta Part A*, 130(2014)302.
25. A.M. Abdelghany, E.M. Abdelrazek, S.I. Badr, M.A. Morsi, *Materials and Design*, 97(2016)532.

26. P. B. Bhargav, B. A. Sarada, A. K. Sharma and V. V. R. N. Rao, *J. Macromolecular Science, Part A: Pure and Appl. Chem.*, 47 (2010) 131.
27. S. Mahendia, A. K. Tomar and S. Kumar, *Journal of Alloys and Compounds*, 508 (2010) 406.
28. N.A. El-Ghamaza, M.A. Diabb, A.Z. El-Sonbatib, O.L. Salem, *Spectrochimica Acta Part A*, 83 (2011) 61.
29. P. Kuivalainen, H. Stubb, H. Isotalo, P. Yli and C. Holmstrom, *Phys. Rev. B*, 31 (1985) 7900.
30. J.L. Bredas, R.R Chance, R. Silbey, *Phys. Rev. B*, 26 (1982) 5843.
31. S. Kivelson, *Phys. Rev. B*, 25 (1982) 3798.
32. N.F. Mott and R.W. Gurney, *Electronic processes in Ionic crystals* (London: OUP) 1940 P. 34.
33. S. Kivelson, *Phys. Rev. Lett.*, 46 (1981) 1344.
34. R. Hasegawa, Y. Takahashi, Y. Chatani, H. Tadakora, *Polym. J.*, 13 (1972) 600.
35. C.H.V.V. Ramana, A.B.V. Kiran Kumar, A. Satya Kumar, M. Ashok Kumar, M.K. Moodely, *Thermochim. Acta*, 566 (2013) 130.
36. T. Sankarappa, M. Prashant Kumar, G.B. Devida, N. Najaraja, R. Ramakrishnareddy, *J. Mol. Struct.*, 88 (2008) 308.
37. S.E. Hao, L. Sun, J. Huang, *Matter. Chem. Phys.*, 109 (2008) 45.
38. S. Ramesh, A. H. Yahaya and A. K. Arof, *Solid State Ionics*, 153 (2002) 291.
39. J. A. Campbell, A. A. Goodwin and G. P. Simon, *Polymer*, 42 (2001) 4731.
40. C. Tsonos, L. Apekis, K. Viras, L. Stepanenko, L. Karabanova and L. Sergeeva, *Solid state Ionics*, 143 (2001) 229.
41. Z. M. Dang, Y. H. Zhang and S. C. Tjong, *Synth. Metals*, 146 (2004) 79.
42. C. Tsonos, L. Apekis, K. Viras, L. Stepanenko, L. Karabanova and L. Sergeeva, *Solid state Ionics*, 143 (2001) 229.
43. C. C. Ku and R. Liepuns, *Electrical Properties of Polymers*, Hanser Publish. New York, 1987.
44. L. Pacal, L. Linets, V. S. Kov and V. Dusheiko, *Solid state Ionics*, 147 (2002) 383.
45. N. El-Ghamaz, M. Diab, M.S. Zoromba, A. El-Sonbati, O. El-Shahat, *Solid State Sci.*, 24 (2013) 140.
46. R. D. Sherman, L. M. Middleman, S. M. Jacobs, *Polymer Engineering and Science*, 23(1)(1983)36.

© 2016 The Authors. Published by ESG (www.electrochemsci.org). This article is an open access article distributed under the terms and conditions of the Creative Commons Attribution license (<http://creativecommons.org/licenses/by/4.0/>).